Industrial Chemistry & Materials

ROYAL SOCIETY OF CHEMISTRY

PAPER

View Article Online
View Journal

Cite this: DOI: 10.1039/d6im00110f

Hemicellulose integration enhances lignin valorization to sustainable high-performance potassium fulvic-like fertilizer

Kaixia Liang,[a] Jiale Yu,[a] Jialong Lv,[d] Qi Tang,[a] Zhiqian Meng,[a] Meng Liu,[a] Zhimin Chen,[ac] Lihang Guan,[ac] Qinqin Xia,[a] Shuo Dou,[a] Xiaoxue Song,[b] Haipeng Yu *[a] and Yongzhuang Liu *[ac]

Global agricultural sustainability faces dual threats from inorganic fertilizer overuse and soil organic matter degradation. To address this, we developed a catalytic-hydrothermal humification process that transforms lignin into high-performance potassium fulvic-like (KFA) fertilizers. Using organosolv pulping, we elucidated the structure–function relationship between lignin and derived KFA fertilizers. Optimized organosolv processing (160 °C, 4 h) yielded divergent lignins: acid-catalyzed ethanosolv (AEL-7/3, 96.16% yield) and base-catalyzed ethanosolv (NEL-3/7, 93.01% yield). Spectral and compositional analysis revealed exclusive hemicellulose incorporation in NEL-3/7. Subsequent catalytic-hydrothermal humification (140 °C, 2 h) demonstrated that potassium fulvic-like substances from hemicellulose-containing lignin (NEL-3/7) met all parameters (fulvic acid (FA), K_2O, moisture, insolubles, pH) of bio-based potassium fulvate standards and even surpassed fossil-based equivalents. Crucially, hemicellulose integration enhanced conversion to small-molecular acids bound to lignin, boosting the FA content to 54.93%—confirming its superior functionality in FA formation. This strategy establishes a sustainable pathway for structure-guided lignin valorization into fertilizers, reducing agriculture's reliance on non-renewable resources while enabling green plant growth.

Keywords: Potassium fulvic-like fertilizer; Lignin valorization; Hemicellulose integration; Catalytic humification; Structure–performance relationship.

Received 1st April 2026,
Accepted 5th May 2026

DOI: 10.1039/d6im00110f

rsc.li/icm

1 Introduction

Rapid population growth and economic development exert immense pressure to enhance agricultural yields and quality, driving a significant global surge in fertilizer demand. As essential plant growth regulators,[1] fertilizers primarily comprise inorganic (*e.g.*, urea)[2] and organic types.[3] However, the rampant overuse of traditional inorganic fertilizers has exacerbated soil burdens, disrupting the soil aggregate structure, causing compaction, erosion, and salinization.[4] This leads to severe soil organic matter (SOM) loss, diminished soil fertility, impaired plant nutrient uptake, and ultimately, reduced crop yields. Consequently, transitioning from traditional inorganic fertilizers to organic plant growth regulators is imperative for sustaining soil fertility and ensuring agricultural sustainability.

SOM represents the highly dynamic organic fraction of soil.[5] Humic substances (HS), the bioactive component of SOM,[6] consist primarily of humic acid (HA), fulvic acid (FA), and the highly condensed, inert humin.[7] FA, characterized by its low molecular weight and higher abundance of functional groups (*e.g.*, carboxyl and phenolic hydroxyl groups) compared to HA,[8] exhibits metal chelation properties that can reduce plant uptake of heavy metals.[9] As a potent plant growth stimulant, FA is also crucial for maintaining soil stability.[10] Additionally, HS are not only naturally present in soil[6] and river sediments,[11] but researchers have also performed sequential extraction of HA from soil sediments and systematically analyzed their molecular markers to elucidate the diverse composition of SOM, with the results indicating that the investigated humic acids originated from terrestrial plants.[12] Researchers can also extract FA from sources such as lignite and weathered

[a] State Key Laboratory of Woody Oil Resources Utilization, Key Laboratory of Bio-based Material Science and Technology of Ministry of Education, Northeast Forestry University, Harbin 150040, China. E-mail: yuhaipeng20000@nefu.edu.cn, lyz@nefu.edu.cn
[b] College of Home and Art Design, Northeast Forestry University, Harbin 150040, China
[c] School of Future Technology, Northeast Forestry University, Harbin 150040, China
[d] Tangshan Green Chemical Industry Technology Research Institute, Tangshan Sanyou Chemical Industry Co., Ltd., Tangshan 063305, China

coal. Li *et al.*[13] utilized H_2O_2 and KOH to oxidize lignite for FA production, while Zhou *et al.*[14] developed an electro-oxidation strategy to convert coal-based HA into FA. However, whether relying on non-renewable mineral resources or the slow formation of natural HS, both approaches struggle to meet the demands of modern agriculture for efficient and sustainable FA production.

Traditionally, HS are widely present in nature and rely on the decay or chemical transformation of plant or microbial residues.[15] Essentially, they represent products of the continuous degradation and cycling of plant-derived organic matter under environmental conditions. Plant residues serve as the primary initial source of SOM, which undergoes transformation and stabilization into SOM through a complex decomposition process mediated by soil microorganisms. Research indicates that FA/HA in soil may primarily originate from the degradation of terrestrial plant metabolites and residues.[16] Furthermore, the soil environment can accelerate the humification process of wheat straw by promoting HS formation.[17] However, the natural humification process of plant residues—being inherently slow and susceptible to environmental variations—is inadequate to meet modern agriculture's demand for efficient and balanced nutrient supply. Therefore, establishing a synergistically coupled production system that integrates sustainable biomass utilization with artificial humification technology represents a crucial approach to ensuring the long-term sustainable output of fulvic acid.

Recent approaches to produce FA from biomass have often employed traditional composting. For instance, adding trace amounts of molecular sieves significantly enhanced humification during composting, increasing the HA content by 18.1% and the HA/FA ratio by 59.6% after 35 days.[18] Zhou *et al.*[19] reported a 17.83% FA yield from cattle manure compost using a KOH–H_2O_2 oxidation system. However, composting requires specific environmental conditions (temperature, humidity, pH) and is inherently slow. Similarly, anaerobic digestion—the bacterial breakdown of biomass in oxygen-free environments to produce biogas and digestate[20]—allows HS extraction (*e.g.*, *via* acid extraction) from the digestate. Digestate-derived HS exhibit superior biostimulant properties compared to commercial HS from lignite.[21] Like composting, anaerobic digestion is highly sensitive to the substrate type and composition, requires strict temperature and pH control, and is constrained by environmental factors. Therefore, exploring more efficient and flexible methods is essential.

Alkaline hydrothermal treatment of biomass waste facilitates humification, yielding hydrothermal humic acid.[22] For example, hydrothermal pretreatment of xylose residues yielded FA concentrations up to 9.6 g L^{-1}.[7] Co-hydrothermal humification of strongly alkaline solid waste carbide slag and cotton stalk achieved a maximum HA yield of 19%.[23] Pan *et al.*[24] combined microbial treatment with hydrothermal processing of rice straw to produce FA. Combining hydrothermal humification with biological fermentation under low alkalinity yielded FA conversion rates up to 39% from rice straw.[25] While hydrothermal treatment improves biomass utilization, its efficiency is highly temperature-dependent; excessive temperatures increase environmental burdens. Consequently, overcoming the low FA yields inherent to hydrothermal treatment alone is necessary. Utilizing catalytic methods to synthesize artificial HS from biomass or non-biomass resources represents a highly promising strategy. Fenton reagents show significant potential in assisting neutral hydrothermal humification of lignocellulosic biomass for FA synthesis.[26] Cai *et al.*[8] achieved an FA yield of 25.5 ± 4.3 wt% from *Enteromorpha prolifera via* $FeSO_4{\cdot}7H_2O$ and H_2O_2-induced hour-level humification. Potassium persulfate-hydrothermal co-activation enabled hour-level humification of sawdust to produce FA-like fertilizers.[27] Cai *et al.*[28] treated sugarcane filter cake with calcium hydroxide-activated potassium persulfate, achieving an FA yield of 316.8 mg g^{-1}. Alkaline $FeCl_3$-catalyzed low-temperature pyrolysis of bamboo powder yielded artificial FA at 25.96 ± 1.24 wt% with a high Cd^{2+} immobilization rate of 51%.[29] Collectively, catalytic combined with alkaline hydrothermal treatment synergistically promotes biomass pyrolysis, enhances catalytic efficiency, and offers dual potential for boosting FA yields and remediating soil heavy metal contamination.

Lignin, a major by-product of the pulp and paper industry, remains predominantly utilized through low-value combustion, leading to the waste of significant renewable aromatic resources. Although considerable research has been devoted to the high-value conversion of biomass[30] in recent years, in-depth exploration of papermaking waste remains limited, and the full potential of lignin is far from being realized. From a molecular structural perspective, lignin—the most abundant natural aromatic polymer in nature, composed of *p*-hydroxyphenyl (H), guaiacyl (G), and syringyl (S) units[31]—features a benzene-ring-rich backbone and phenolic hydroxyl groups that exhibit significant structural similarity to the aromatic core units of FA (Scheme 1a). This inherent structural homology provides a theoretical foundation for the targeted conversion of lignin into fulvic-like substances. However, systematic investigations into the direct preparation of fulvic-like materials from lignin *via* controlled chemical modification strategies remain scarce.

To this end, this study established a strategy that integrates papermaking with the high-value utilization of pulping by-product lignin, aiming to achieve the comprehensive fractionation and high-value utilization of all components of the lignocellulosic feedstock. The strategy initially involves the selective fractionation of poplar wood under mild conditions using an acidic ethanol (AE) or basic ethanol (NE) system, where the reaction temperature and time were optimized based on the lignin yield. This process concurrently yields cellulose pulp—suitable for papermaking or saccharification fermentation—while separating the pulping by-products, namely acid-catalyzed ethanol lignin (AEL) or base-catalyzed ethanol lignin (NEL). Crucially, the

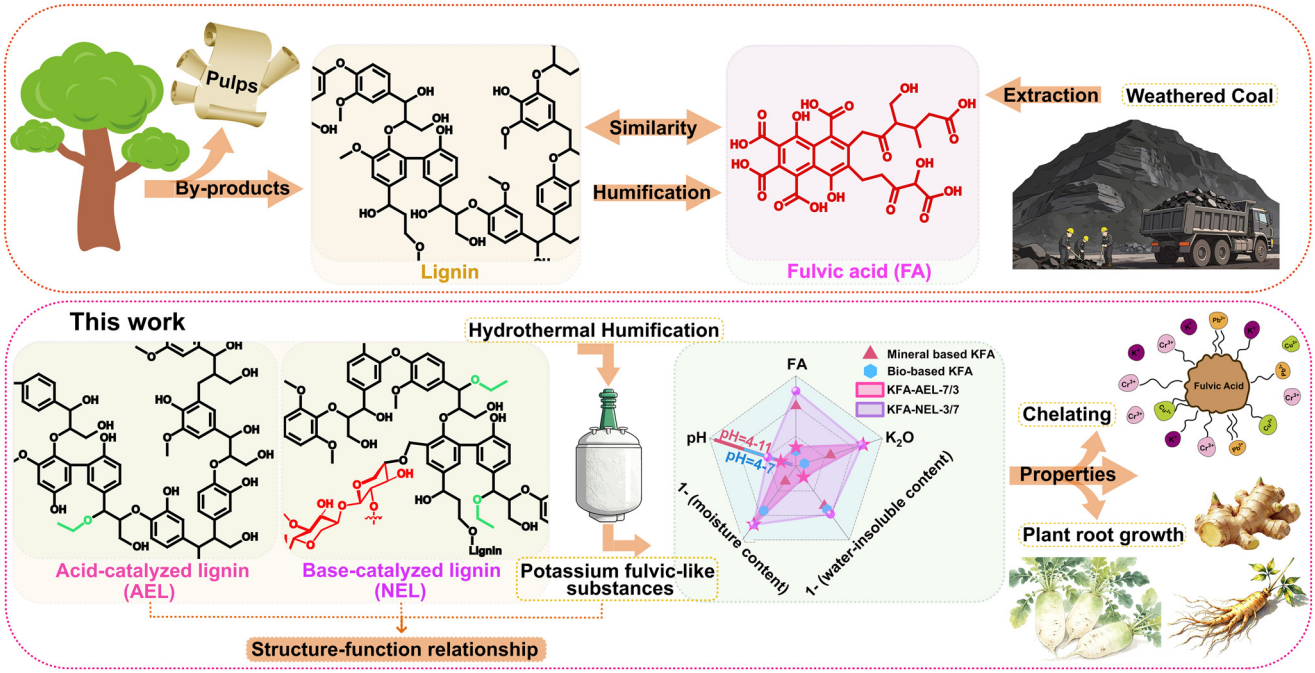

Scheme 1 Synthesis of lignin-based potassium fulvic-like substances *via* humification. (a) Preparation of fulvic acid from pulping by-products *versus* that from weathered coal; (b) structure–function relationship investigations of organosolv lignin-based potassium fulvic-like fertilizer and key parameters in this work.

isolated lignin, which shares a natural structural similarity with FA (characterized by a benzene-ring-rich skeleton and phenolic hydroxyl groups), serves as an ideal molecular scaffold for constructing the aromatic core of humic substances. Based on this, a catalytic synergistic alkaline hydrothermal treatment strategy was further employed to convert AEL and NEL into potassium fulvic-like (KFA) substances, with the process conditions optimized using FA content as the key indicator to obtain the optimal preparation protocol; the resulting KFA products were systematically evaluated against all key parameters (FA content, K_2O content, moisture, water-insoluble matter, and pH) specified in the HG/T 5334-2018 standard. Crucially, we analyzed the lignin purity, molecular weight, and structure (particularly the impact of xylan incorporation identified in NEL-3/7) to elucidate their influence on the FA yield

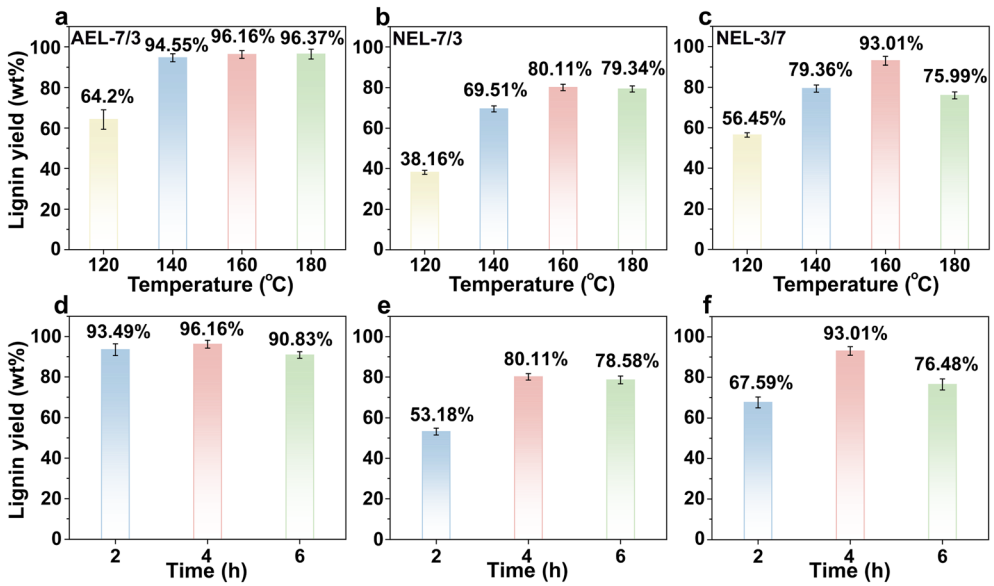

Fig. 1 Separation efficiency of poplar lignin extraction *via* acidic/basic ethanol systems. Fixed time (4 h), varying temperature (120–180 °C): (a) AEL-7/3, (b) NEL-7/3, and (c) NEL-3/7; fixed temperature (160 °C), varying time (2–6 h): (d) AEL-7/3, (e) NEL-7/3, and (f) NEL-3/7.

(Scheme 1b). This controlled synthetic route ultimately yields high-performance potassium fulvic-like fertilizers, which are characterized by a robust aromatic skeleton, abundant surface functional groups, excellent chemical reactivity, and potential biostimulant activity, thereby providing a foundational reference for the high-value conversion of lignin into potassium fulvic-like substances.

2 Results and discussion

2.1 Lignin extraction efficiency

We first investigated the influence of temperature and reaction time on poplar wood powder fractionation efficiency, analyzing the lignin yield (mass ratio of precipitated lignin to original lignin content in the substrate; poplar lignin content = 19.8%). It is worth noting that the ethanol/water ratio (7/3) in the acidic ethanol (AE) system was primarily selected based on the established literature[32] with slight modifications. In contrast, the ratios for the basic ethanol (NE) systems were determined through systematic optimization experiments (Fig. 1b, c, e and f and S1). At a fixed reaction time of 4 h (Fig. 1a–c), the lignin yield in the acidic ethanol (AE) system increased from 64.2% at 120 °C to 96.16% at 160 °C, indicating enhanced solvent diffusion and lignin solubilization with heating.[33] Further temperature increases to 180 °C yielded no significant improvement, establishing 160 °C as the optimal temperature for economic efficiency. Subsequently, varying the reaction time at 160 °C revealed a yield maximum at 4 h (Fig. 1d–f). Prolonged reaction times (>4 h) reduced yields, attributed to excessive lignin degradation and fragmentation under sustained acidic conditions, hindering precipitation. In the basic ethanol (NE) systems (Fig. 1b and c and S1a), the lignin yield also generally increased with temperature up to 160 °C but decreased significantly at 180 °C (NEL-7/3-180-4: 79.34%, NEL-1/1-180-4: 77.29%, NEL-3/7-180-4: 75.99%). While NaOH effectively degrades fibers and solubilizes lignin, excessive temperature promotes degradation into low-molecular-weight fragments stabilized by ethanol, preventing aggregation and precipitation.[34] Time optimization at 160 °C confirmed 4 h as optimal (NEL-7/3-160-4: 80.11%, NEL-1/1-160-4: 80.93%, NEL-3/7-160-4: 93.01%, Fig. 1e and f and S1b). Thus, 160 °C for 4 h was established as the optimal conditions. Under these conditions, maximum yields were: AE system (AEL-7/3: 96.16%); NE systems (NEL-7/3: 80.11%, NEL-1/1: 80.93%, NEL-3/7: 93.01%). These optimal samples were designated as AEL-7/3, NEL-7/3, NEL-1/1, and NEL-3/7 for further analysis.

2.2 Lignin molecular weight determination

The weight-average (Mw) and number-average (Mn) molecular weights and polydispersity index (PDI = Mw/Mn) of the isolated lignins are shown in Fig. 2a and Table S1. Lignin from the AE system (AEL-7/3) exhibited the highest Mw (1977 g mol^{-1}) and broadest distribution (PDI = 3.6), indicative of structural heterogeneity. This aligns with reports that strong acid conditions promote condensation reactions, forming larger, more complex lignin fragments.[35] Lignins from the NE systems (NEL-7/3, NEL-1/1, NEL-3/7) showed lower Mw

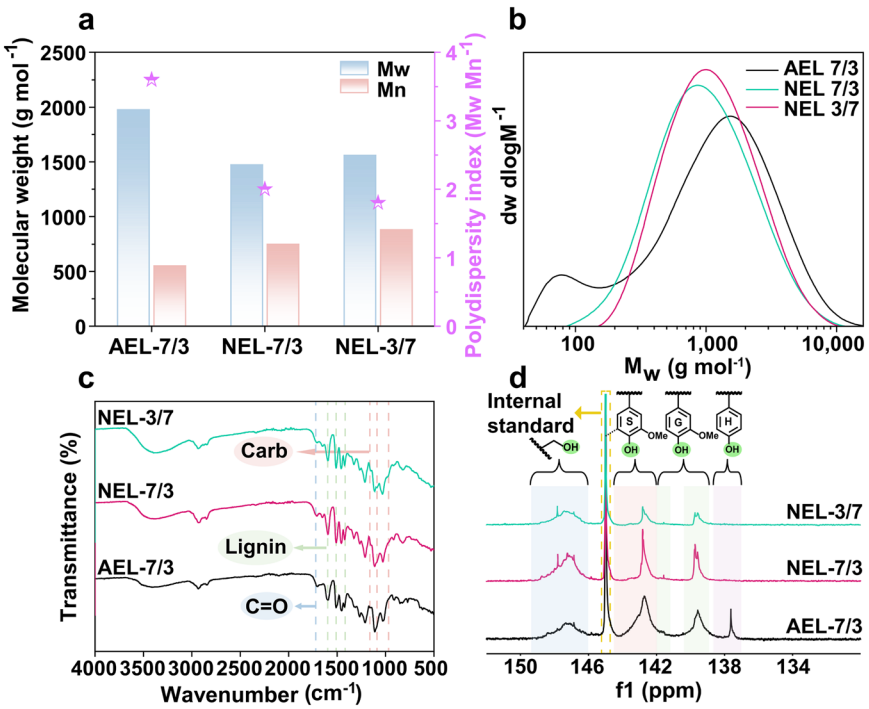

Fig. 2 Structural analysis of lignin from different systems. (a) Molecular weight (Mw) and polydispersity index (Mw/Mn) of lignin; (b) molecular weight distribution curve; (c) FT-IR spectra; (d) ^{31}P NMR spectra.

(1474, 1071, 1559 g mol^{-1}, respectively) and significantly lower PDI, suggesting narrower molecular weight distributions and better homogeneity (Fig. 2b). Uniform molecular weight distribution may be advantageous for subsequent fulvic acid conversion.

2.3 Structural characterization of lignin

FT-IR spectroscopy (Fig. 2c and S2a) confirmed characteristic lignin bands: broad O–H stretching (3000–3600 cm^{-1}), C–H stretching of $–CH_3$/$–CH_2–$ (2932, 2838 cm^{-1}), C═O stretching (1704 cm^{-1}), and aromatic skeletal vibrations (1601, 1510, 1425 cm^{-1}). Critically, the spectra of NEL-3/7 and NEL-1/1 revealed signals associated with residual hemicellulose (xylan): C–O stretching in glycosidic bonds (~1160 cm^{-1}), C–O/C–C stretching and xylan glycosidic bonds (~1050 cm^{-1}), and C–O–C asymmetric stretching (~970 cm^{-1}).[36] This provided preliminary evidence of xylan incorporation within these lignin isolates.

^{31}P NMR analysis (Fig. 2d and S2b, Tables 1 and S2) quantified hydroxyl groups: aliphatic OH (146–149 ppm), carboxylic acid (–COOH, 134.2–135.5 ppm), and phenolic OH subtypes (S-unit: 142.17–144.5 ppm, G-unit: 141.42–142.17 ppm & 138.79–140.17 ppm, H-unit: 137.1–138.4 ppm).[37] AEL-7/3 displayed a higher phenolic OH content (4.92 mmol g^{-1}) and a lower aliphatic OH content (1.78 mmol g^{-1}) compared to NE lignins. This reflects acid-catalyzed dehydration and cleavage of β-O-4 aryl ether bonds under acidic conditions, exposing more phenolic groups,[38] consistent with 2D HSQC NMR findings. Conversely, the ethanol–water solvent in NE systems better preserved lignin side chains and β-O-4 linkages, resulting in higher aliphatic OH and lower phenolic OH contents, as confirmed by 2D HSQC NMR.

2D HSQC NMR analysis (Fig. 3 and S3) provided detailed structural insights. Semi-quantification of inter-unit linkages revealed stark differences: NE lignins (NEL-7/3, NEL-1/1, NEL-3/7) exhibited similar linkage profiles, while AEL-7/3 showed significantly reduced β-O-4′ and β-β′ linkages, with the β-5′/α signal being absent. This confirms extensive acid-catalyzed cleavage of aryl ether bonds, corroborating the ^{31}P NMR data. Ethanol incorporation as ethoxyl groups[39] was evident in all lignins *via* characteristic cross-signals (*e.g.*, $\delta C/\delta H$ 64/3.55 ppm). Crucially, xylan signals[40] were distinctly observed in NEL-3/7 and NEL-1/1 ($\delta C/\delta H$ 70.55/3.06, 74.14/3.28, 77.42/3.48 ppm), confirming incomplete separation from hemicellulose. This difference can be primarily attributed to the distinct characteristics of the extraction systems: during lignin extraction using the acidic ethanol (AE) system, acid hydrolysis completely degrades hemicellulose into monosaccharides and further decomposition products, which are readily removed in subsequent purification steps such as precipitation and washing; in contrast, the milder basic ethanol (NE) systems result in incomplete separation of lignin from hemicellulose, with the latter retained mainly in the form of lignin–carbohydrate complexes (LCCs). Lignin purity analysis (using the NREL method, Fig. S4a) showed that AEL-7/3 had a purity of 91.85%, and NEL-7/3 had 85.6% (influenced by acid-soluble lignin), while the purities of NEL-1/1 and NEL-3/7 dropped to approximately 70%, attributable to both acid-soluble lignin and xylan incorporation (validated by HSQC). Additionally, analysis of lignin yields across different systems (Fig. 1 and S1) demonstrates that under the same optimal conditions (160 °C, 4 h), the yield of NEL-3/7 reaches 93.01%, whereas that of NEL-1/1 decreases to approximately 80%. Therefore, based on the yield and purity, AEL-7/3 (high yield and high purity), NEL-7/3 (higher purity), and NEL-3/7 (high yield with xylan incorporation) were selected for fulvic acid conversion, while NEL-1/1 was excluded due to its low yield and purity.

2.4 Efficiency of KFA production *via* catalytic-hydrothermal humification

To systematically validate the accuracy of the analytical method, methodological validation was conducted according to the Chinese industry standard HG/T 5334-2018, using an FA analytical standard (85% purity) as the reference material (Fig. S7). FA standard solutions at varying concentrations (1#: 0.68 mg mL^{-1}, 2#: 1.7 mg mL^{-1}, 3#: 10.2 mg mL^{-1}, 4#: 17 mg mL^{-1}, 5#: 34 mg mL^{-1}) were employed as substrates to evaluate the method's accuracy and stability across different concentration levels. All experiments were performed in triplicate to ensure reproducibility and statistical reliability. The validation results (Fig. S7) demonstrate that under varying substrate concentrations, accuracy consistently ranged from 97.67% to 99.43%, indicating excellent method accuracy and robust concentration adaptability. These findings confirm the analytical method's reliability and establish a solid foundation for precise FA quantification in subsequent potassium fulvic-like samples.

In this study, NEL-7/3 was first employed as a model substrate to systematically investigate reagent effects on fulvic acid (FA) generation during humification. 10.3% of NEL-7/3 was identified as FA according to the HG/T

Table 1 Quantitative analysis of lignin functional groups by ^{31}P NMR

Lignin sample	Aliphatic OH, mmol g^{-1}	Phenolic OH, mmol g^{-1}			COOH, mmol g^{-1}
		Syringyl	Guaiacyl	*p*-Hydroxy phenyl	
AEL-7/3	1.78	2.95	1.62	0.35	—
NEL-7/3	4.34	2.02	1.66	—	—
NEL-3/7	2.44	0.89	0.69	—	—

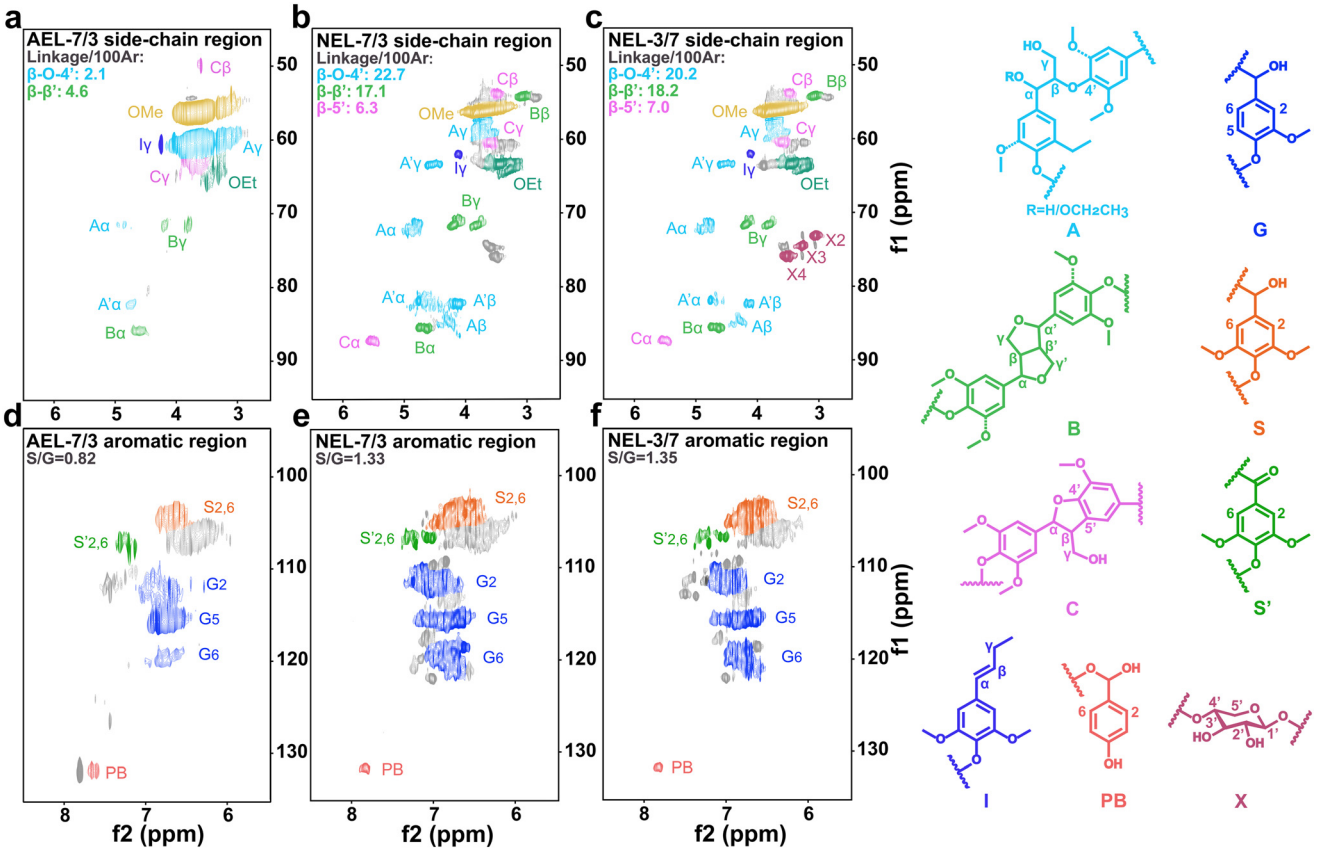

Fig. 3 2D HSQC NMR structural features of lignins from different systems. (a–c) Side-chain region; (d–f) aromatic region.

5334-2018 standard; KOH addition alone increased the FA content to 19.98%, whereas KOH with paraformaldehyde reduced it to 16.08%. When KOH was combined with sodium metabisulfite, the FA content significantly rose to 37% – meeting the HG/T 5334-2018 requirement (>35%) – demonstrating sodium metabisulfite's marked promotion of FA formation. Further addition of paraformaldehyde to the KOH/sodium metabisulfite system increased the FA content to 49.44% (Table S4), indicating that sulfate compounds significantly enhance FA generation.

Subsequently, Kraft lignin was used to screen sulfate compounds (Table S5). About 22% of the Kraft lignin was identified as FA using the HG/T 5334-2018 standard. Sodium sulfate (Na_2SO_4) showed no significant humification promotion (FA content: 21.55%). In contrast, sodium metabisulfite ($Na_2S_2O_5$) significantly elevated the FA content to 44.46%. Although sodium sulfite (Na_2SO_3) yielded a comparable FA content (41.12%), the resulting potassium fulvic-like product's water-insoluble content (5.7%) exceeded the standard limit (≤5%). Thus, sodium metabisulfite was identified as the optimal reagent.

A possible mechanism for the humification process is proposed: under high-temperature conditions, lignin dissolves in KOH solution with activated hydroxyl groups, while paraformaldehyde-mediated hydroxymethylation[41] and oxidation by residual air synergistically drive potassium fulvic-like substance formation. During this process, sodium metabisulfite ($Na_2S_2O_5$) hydrolyzes in alkaline aqueous solution to form sodium bisulfite ($NaHSO_3$), releasing high concentrations of sulfite (SO_3^{2-}) and bisulfite (HSO_3^-) ions. These nucleophilic species attack reactive lignin sites (*e.g.*, β-O-4′ aryl ether bonds), facilitating sulfonic acid group introduction[42] – which enhances product water solubility and imparts excellent amphiphilic properties to potassium fulvic-like substances. Although fulvic acid formation requires an alkaline environment, excessively high pH promotes lignin fragment repolymerization. Sodium metabisulfite exhibits weak acidity during hydrolysis, acting as an *in situ* buffer that moderates alkalinity and stabilizes the reaction environment within the optimal weakly alkaline-to-alkaline range for sulfonative degradation. In contrast, sodium sulfite (Na_2SO_3) solution is inherently alkaline and lacks pH-regulating capacity, leading to an elevated water-insoluble content in the product. This is primarily because strong alkalinity promotes paraformaldehyde-induced hydroxymethylation, causing lignin cross-linking and a molecular size increase (explaining the FA content decrease observed with KOH/paraformaldehyde in Table S4), thereby reducing water solubility. In summary, sodium metabisulfite both supplies nucleophiles to promote sulfonation and optimizes the acid–base environment,

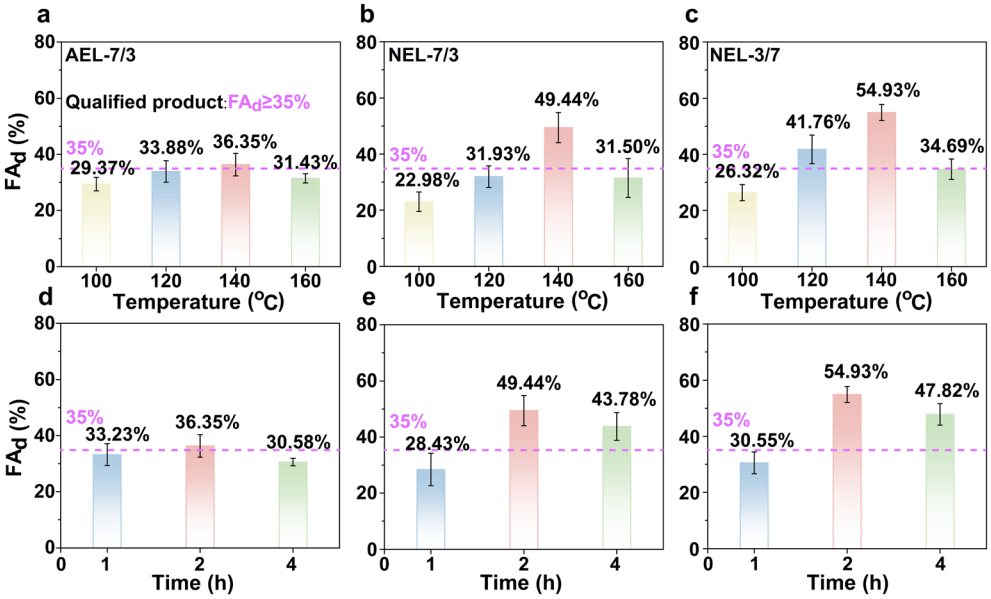

Fig. 4 Efficiency of lignin conversion to fulvic acid (FA). Fixed time (2 h), varying temperature (100–160 °C): (a) AEL-7/3, (b) NEL-7/3, and (c) NEL-3/7; fixed temperature (140 °C), varying time (1–4 h): (d) AEL-7/3, (e) NEL-7/3, and (f) NEL-3/7.

synergistically enabling efficient potassium fulvic-like substance generation.

The influence of temperature and time on fulvic acid (FA) content in potassium fulvic-like (KFA) was evaluated, alongside key parameters (K_2O, moisture, water-insoluble matter, pH) against the HG/T 5334-2018 standard. At a fixed time (2 h, Fig. 4a–c), the FA content increased from 100 °C to 140 °C. Elevated temperature enhances lignin dissolution in KOH, hydroxyl group activation, paraformaldehyde-mediated hydroxymethylation,[41] and oxidation by residual O_2, driving fulvic acid formation. However, the FA content decreased at 160 °C. Under alkaline hydrothermal conditions, O_2 generates reactive oxygen species ($O_2\cdot^-$, HOO·, HOO^-).[43] High temperature enhances nucleophilic attack by HOO^- on low-electron-density sites (*e.g.*, carbonyl carbons) in lignin, leading to irreversible ring-opening and aliphatic carboxylate formation. Although the reductant $Na_2S_2O_5$ was present, it could not fully prevent this degradation. $Na_2S_2O_5$ also plays a key role in sulfonating lignin, enhancing water solubility[42] and contributing to the amphiphilic nature of FA. The FA content peaked at 140 °C: KFA-AEL-7/3-140-2: 36.35%; KFA-NEL-7/3-140-2: 49.44%; KFA-NEL-3/7-140-2: 54.93% (all meeting the HG/T 5334-2018 FA standard, though KFA-AEL-7/3-140-2 was marginal). The lower reactivity of AEL-7/3 correlates with its structural features (high phenolic OH, low aliphatic OH), which confer greater antioxidant capacity.[44] The superior FA yield from NEL-3/7 is attributed to the incomplete separation of lignin from hemicellulose, which is predominantly retained in the form of lignin–carbohydrate complexes (LCCs) (*i.e.*, incorporated xylan). Under alkaline conditions, xylan hydrolyzes to xylose, dehydrates to furfural, and hydrates to levulinic acid; these small-molecule acids bind to lignin fragments, facilitating FA formation.[45] Time optimization at 140 °C (Fig. 4d–f) showed that the FA content peaked at 2 h and decreased at 4 h due to over-oxidation. Only a trace amount of lignin was identified as FA (AEL-7/3: 5.03%; NEL-7/3: 10.3%; NEL-3/7: 6.4%) (Fig. S4b, Table S4), all significantly below the HG/T 5334-2018 threshold (>35%), confirming that the proportion of lignin identifiable as FA in the starting materials is extremely low. Thus, 140 °C for 2 h was optimal for conversion, with products designated as KFA-AEL-7/3, KFA-NEL-7/3, and KFA-NEL-3/7. Notably, although the acidic ethanol (AE) system achieves a higher lignin separation yield than the basic ethanol (NE) systems, this yield reflects only the isolated lignin quantity and does not correlate with its reactivity in potassium fulvic-like substance conversion. These results demonstrate that for high-performance potassium fulvic-like materials, lignin precursor quality—specifically structural amenability to conversion—is far more critical than separation efficiency.

2.5 Structural characteristics of KFA

X-ray photoelectron spectroscopy (XPS) (Fig. 5a–f and S5) analyzed surface chemistry. C 1s spectra were deconvoluted into: C–C/C–H (284.8 eV), C–O/C═O (286.5 eV), O–C═O (288.5 eV),[46] and K 2p satellites (292.8 eV, 295.6 eV).[47] O 1s spectra showed: C═O (531.5 eV), C–O (532.3 eV), and C–OH (533.0 eV).[26] KFA from NE systems (KFA-NEL-7/3, KFA-NEL-3/7) exhibited significantly lower C–C contents (45.26%, 37.24%) than their parent lignins (61.56%, 46.18%), indicating oxidation. KFA-AEL-7/3 showed minimal C–C reduction (42.34% *vs.* AEL-7/3: 44.09%), consistent with its structural stability and lower reactivity. KFA-NEL-3/7 displayed the highest

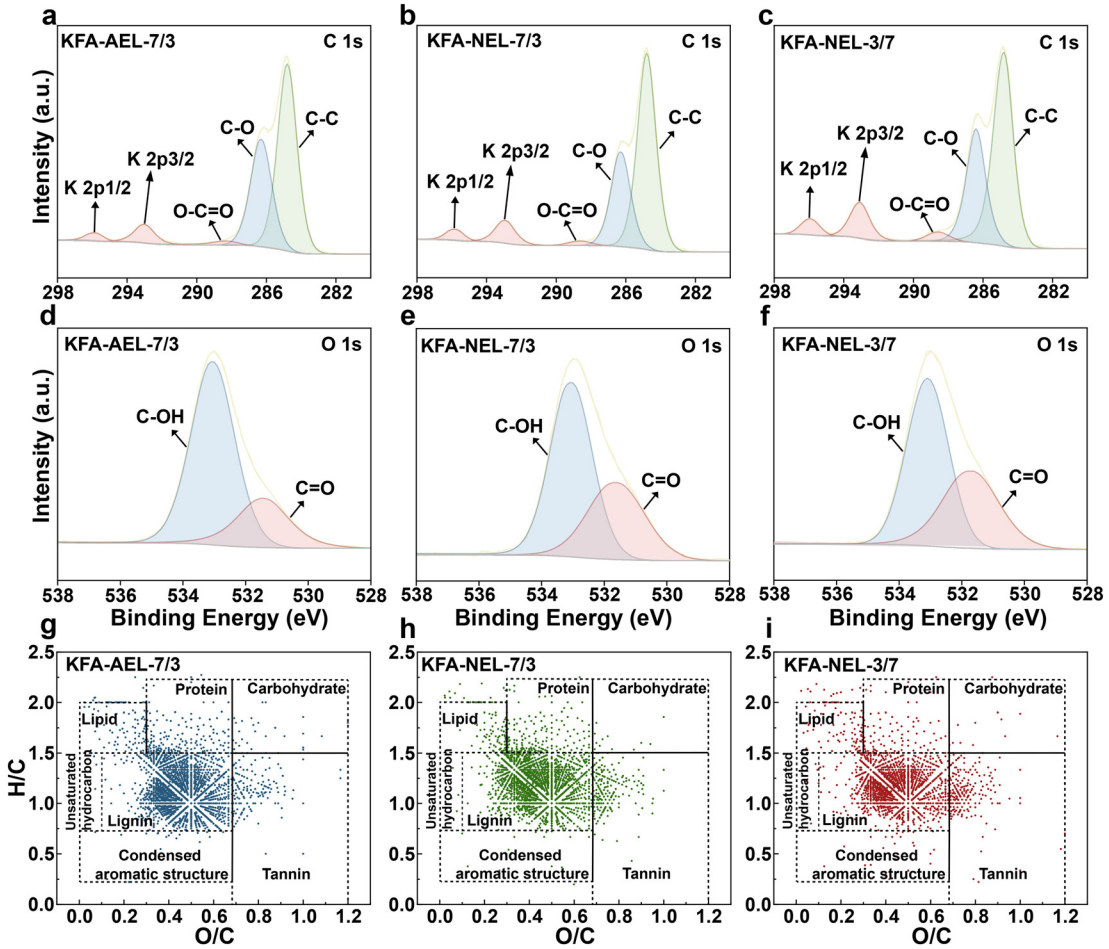

Fig. 5 Structural investigations of lignin-based KFA. XPS spectra (a–f) illustrating the structural evolution from lignin to KFA (focus on C 1s and O 1s regions showing key functional group changes); Van Krevelen diagrams (g–i) of KFA in different systems plotted based on H/C and O/C distributions.

C═O content (16.09%), significantly exceeding KFA-AEL-7/3 (6.77%) and KFA-NEL-7/3 (9.57%). This supports the role of incorporated xylan in NEL-3/7 generating small-molecule acids that bind to lignin fragments during FA formation. The emergence of the O–C═O peak in C 1s and the prominent C═O peak in the O 1s spectra for all KFA samples confirm oxidative introduction of carboxyl groups, characteristic of FA. Elemental analysis (Table S3, Fig. S6) revealed lower carbon, higher oxygen content, and higher H/C and O/C atomic ratios in KFA compared to parent lignins. Lower H/C often correlates with higher aromaticity, while higher O/C indicates greater oxygen functionality.[48] Thus, KFA possesses lower aromaticity and richer oxygen-containing functional groups (especially carboxyls) than the precursor lignins. Van Krevelen diagrams (Fig. 5g–i) were constructed based on the H/C and O/C ratios of KFA molecules to characterize their molecular composition. Seven component groups were delineated using these ratios: lipid-like (H/C: 1.5–2.2; O/C: 0–0.3), protein-like (H/C: 1.5–2.2; O/C: 0.3–0.67), carbohydrate-like (H/C: 1.5–2.2; O/C: 0.67–1.2), unsaturated hydrocarbons (H/C: 0.7–1.5; O/C: 0–0.3), lignin-like (H/C: 0.7–1.5; O/C: 0.3–0.67), tannin-like (H/C: 0–1.5; O/C: 0.67–1.2), and condensed aromatics (H/C: 0.2–0.7; O/C: 0–0.67). The results indicate that all KFA samples are predominantly composed of lignin-based structural molecules retaining characteristic benzene ring functional groups, confirming their high structural similarity to lignin. Additionally, the samples exhibit a distribution across all seven regions, attributed to the characteristics of the raw lignin materials. Phong *et al.*[49] extracted fulvic-like substances from sawdust using ionic liquids and found that the extracts contained lignin-like and lipid-like molecules, featuring key organic groups such as aromatic, phenolic, and methoxy moieties. Meanwhile, Mu *et al.*[50] prepared FA *via* hydrothermal treatment of food waste, in which the carboxyl and hydroxyl groups in the structure synergistically imparted good hydrophilicity to the product. Compared with the above reports, the XPS and elemental analysis results of the KFA obtained in this study also revealed abundant oxygen-containing functional groups (especially carboxyl and hydroxyl) as well as retained aromatic structures, confirming its fulvic-like nature. Moreover, the introduction of sulfonic acid groups endows KFA with superior amphiphilic properties, providing experimental evidence for a deeper understanding of the structural diversity of biomass-derived humic substances.

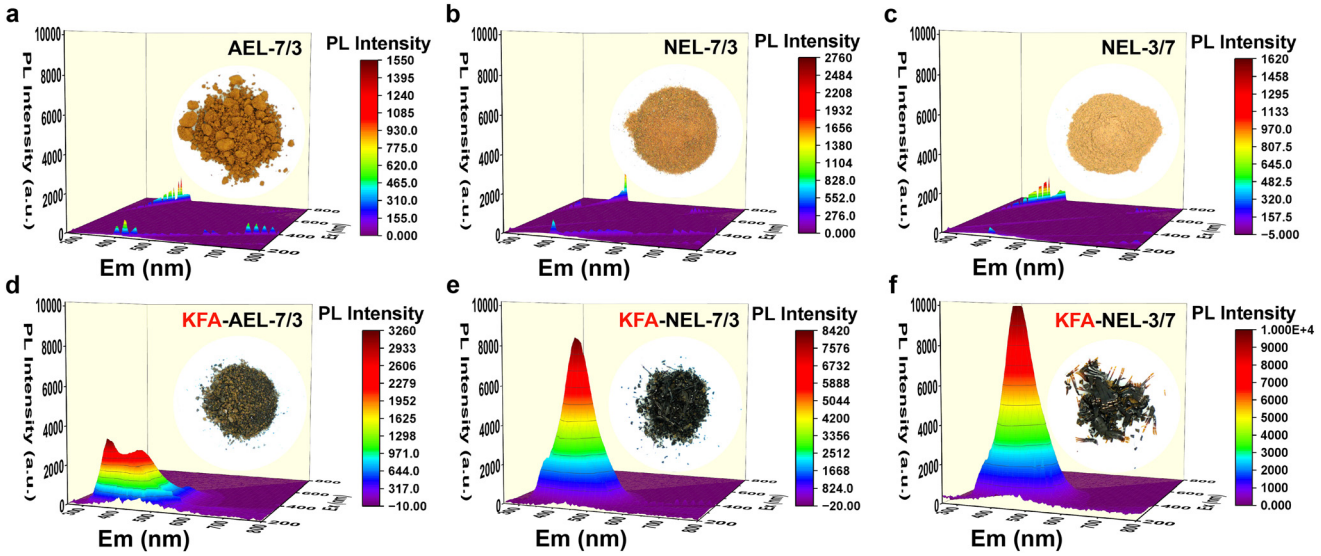

Fig. 6 3D EEM fluorescence spectra of potassium fulvic-like (KFA) substances from different systems. (a–c) Raw lignins; (d–f) corresponding KFA products.

Table 2 Compliance analysis of KFA quality based on the HG/T 5334-2018 standard

Project/sample	FA content (dry basis, %)	K_2O content (dry basis, %)	Water-insoluble matter (dry basis, %)	Moisture (%)	pH (1 : 100)
Bio-based potassium fulvate (standard)	≥35%	≥5%	≤5%	≤5%	4.0–7.0
Mineral-based potassium fulvate (standard)	≥50%	≥8%	≤8%	≤15%	4.0–11.0
Commercial mineral-based potassium fulvate	59.76%	11.00%	7.6%	0.40%	9.7
KFA-AEL-7/3	36.35%	11.78%	31.3%	0.30%	4.7
KFA-NEL-7/3	49.44%	11.73%	3.1%	0.10%	5.6
KFA-NEL-3/7	54.93%	11.63%	1.1%	0.19%	5.3

2.6 Fluorescence characteristics of KFA

Three-dimensional excitation–emission matrix (3D EEM) fluorescence spectroscopy characterized lignin and KFA (Fig. 6). FA typically exhibits characteristic fluorescence peaks within λEx/Em = 200–500/380–550 nm, specifically λEx/Em = 235–255/318–464 nm and λEx/Em = 280–345/320–458 nm.[51] Raw lignins showed minimal fluorescence in this region (Fig. 6a–c), consistent with negligible FA formation during organosolv extraction (Fig. S4b). The fluorescence intensity correlated positively with the FA content (Table 2): KFA-AEL-7/3 < KFA-NEL-7/3 < KFA-NEL-3/7 mirrored the increasing fluorescence intensity trend (Fig. 6d–f). All KFA samples exhibited peaks within λEx/Em = 210–380/330–550 nm (Fig. 6d–f), aligning with typical FA ranges. Combined with their distinct flaky morphology (*vs.* raw lignin), this confirms the successful formation of potassium fulvic-like (KFA) substances.

2.7 Key quality indicators and standard compliance

KFA samples were rigorously evaluated against the HG/T 5334-2018 standard (Table 2). All samples met the moisture (<5%) and pH (4.0–7.0) requirements. The K_2O content significantly exceeded the standard (≥5%), ranging from 11.63% to 11.78%. However, KFA-AEL-7/3 failed the water-insoluble matter requirement (≤5%), exhibiting 31.3%. This is likely due to paraformaldehyde-induced hydroxymethylation causing lignin cross-linking and increased molecular size, reducing water solubility. Crucially, KFA-NEL-7/3 and KFA-NEL-3/7 met all five HG/T 5334-2018 parameters. Notably, lignin containing hemicellulosic components exhibited a higher FA yield after humification (KFA-NEL-3/7: 54.93%, Table 2). Using organosolv lignin as a representative substrate, this validates the structure–humification relationship. Its performance approached that of commercial mineral-derived potassium fulvate (59.76%), with all indicators meeting standard requirements, demonstrating potential as a viable fertilizer substitute. Moreover, the analytical method's accuracy was rigorously validated with an FA analytical standard (Fig. S7), ensuring result reliability. Overall, key indicators of the prepared potassium fulvic-like substances align with commercial products, confirming comparable functionality. Using industrial Kraft lignin as an alternative substrate yielded a product with a 44.46% FA content (Table S5), with all parameters meeting standards, confirming the method's broad applicability. Further introduction of exogenous hemicellulose during Kraft lignin humification increased the FA content to 52.82% – validating that hemicellulose

incorporation significantly promotes FA generation and demonstrating economic feasibility in feedstock selection. The hydrothermal process (mild conditions, short duration, one-step conversion) coupled with applicability to industrial lignin further enhances economic viability (Table S6). In summary, this strategy shows economic and application potential in both feedstock and process design. It highlights lignin–carbohydrate complexes' (LCCs) critical role in humification, provides theoretical and experimental support for lignin valorization, and offers new insights for optimizing biomass refining – establishing a green pathway for high-value lignin utilization. Further research should validate the potassium humate fertilizer's effects on plant growth.

3 Conclusions

This study establishes a catalytic-hydrothermal humification strategy for efficiently converting poplar lignin into potassium fulvic-like (KFA) fertilizers. Optimized organosolv processing (160 °C, 4 h) achieved high lignin yields, with acidic ethanol yielding 96.16% (AEL-7/3) and basic ethanol systems yielding 80.11–93.01% (NEL-7/3 to NEL-3/7). Structural analysis revealed that base-catalyzed ethanol-derived lignins (*e.g.*, NEL-3/7) exhibit superior molecular homogeneity and preserved β-O-4 linkages, while uniquely incorporating hemicellulose-derived xylan. This incorporation critically enhanced subsequent fulvic acid (FA) formation. Under humification conditions (140 °C, 2 h), KFA-NEL-3/7 achieved a 54.93% FA content, significantly outperforming KFA-NEL-7/3 (49.44%) and KFA-AEL-7/3 (36.35%), where performance was limited by acid-condensed structures and antioxidant phenolic groups. All products met HG/T 5334-2018 standards except KFA-AEL-7/3, which exceeded the water-insoluble content limit (31.3% $>$ 5%). Fluorescence intensity confirmed FA formation in all cases.

Adopting the strategic transformation and upgrading of green agricultural inputs as the core strategy represents a key pathway to address global challenges and promote sustainable agriculture. Current commercial humic substances are primarily derived from lignite extraction or organic waste composting. However, lignite is non-renewable, and its overexploitation causes resource depletion and environmental pollution. Composting relies on slow microbial degradation, resulting in long cycles and poor stability due to climatic and feedstock sensitivity. This work successfully upgraded waste lignin—typically incinerated or landfilled—into high-value feedstocks, reducing directional humification from months to hours. Notably, lignin extracted *via* the alkaline ethanol system (NEL-3/7, partially as lignin–carbohydrate complexes, LCCs) achieved a 54.93% FA content after humification, comparable to the commercial FA standard (59.76%). This demonstrates the unique functionality of hemicellulose-integrated lignin in sustainable fertilizer production, establishing a fossil-free pathway to supplant inorganic fertilizers, thereby advancing circular bioeconomy principles in agriculture.

4 Experimental section

4.1 Materials

Poplar wood powder was sourced from Lianyungang, Jiangsu Province, China. Kraft lignin was sourced from UPM Co., Ltd., Germany. Sodium hydroxide (NaOH), potassium hydroxide (KOH), sodium sulfite (Na_2SO_3), absolute ethanol, potassium dichromate ($K_2Cr_2O_7$), sodium tetraphenylborate ($C_{24}H_{20}BNa$), and disodium ethylenediaminetetraacetate (EDTA) were purchased from Aladdin Reagent (Shanghai, China). Sodium metabisulfite ($Na_2S_2O_5$), paraformaldehyde ($HO–(CH_2O)_n–H$), and ammonium iron(II) sulfate hexahydrate ($Fe(NH_4)_2(SO_4)_2·6H_2O$) were obtained from Shanghai Yien Chemical Technology Co., Ltd. 1,10-Phenanthroline monohydrate ($C_{12}H_8N_2·H_2O$) was supplied by Shanghai Yuanye Bio-Technology Co., Ltd. Trisodium phosphate (Na_3PO_4) was purchased from Shanghai Bide Pharmatech Ltd. Analytical chemical grade fulvic acid (85% purity) (CAS: 479-66-3) and a phenolphthalein indicator was acquired from Shanghai Macklin Biochemical Co., Ltd. Sodium sulfate (Na_2SO_4) was purchased from Tianjin Zhiyuan Chemical Reagent Co., Ltd.

4.2 Acidic/basic ethanol fractionation of poplar wood powder and process optimization

Dried poplar wood powder (10 g) was mixed with either H_2SO_4 (0.7 wt%) or NaOH (5 wt%) in ethanol–water solution (solid-to-liquid ratio 1 : 15) in a 300 mL hydrothermal reactor. For the acid-catalyzed ethanol (AE) system, the solvent ratio was ethanol : water = 7 : 3 (v/v). For the base-catalyzed ethanol (NE) system, solvent ratios of ethanol : water = 7 : 3, 1 : 1, or 3 : 7 (v/v) were tested. After thorough mixing, reactions were conducted in a forced-air oven. Reaction temperature (120, 140, 160, 180 °C) and time (2, 4, 6 h) were systematically optimized. Post-reaction, mixtures were cooled and subjected to solid–liquid separation. Solid residues were washed with solvent-matched acid/alkali–ethanol–water mixtures until the filtrate was colorless. Combined filtrates were rotary-evaporated to remove ethanol, acidified to pH = 2 with H_2SO_4, and filtered. The isolated lignin was dried at 45 °C. Lignin samples were named according to the system–acid/base–ethanol : water ratio–temperature–time convention (*e.g.*, AEL-7/3-160-4 denotes acid ethanol lignin obtained at 160 °C for 4 h with ethanol : water = 7 : 3).

4.3 Catalytic-hydrothermal humification of lignin and process optimization

Lignins yielding the highest purity under optimal conditions (160 °C, 4 h) – designated as AEL-7/3 (acidic), NEL-7/3, and NEL-3/7 (basic) – served as substrates. Each lignin was mixed with an aqueous solution containing KOH (11.5 wt%), $Na_2S_2O_5$ (6.75 wt%), and paraformaldehyde ($HO–(CH_2O)_n–H$, 2.7 wt%) at a solid-to-liquid ratio of 1 : 4 in a hydrothermal reactor under an air atmosphere (the amounts of the above reagents are all based on lignin mass). Reactions were performed in a closed autoclave

(YZQR-100, Shanghai Yanzheng Experimental Instrument Co. Ltd., Shanghai), with temperature (100, 120, 140, 160 °C) and time (1, 2, 4 h) optimization. After cooling, the solution was adjusted to pH 4–7 with H_2SO_4 and dried at 60 °C. Potassium fulvic-like (KFA) products were named as KFA-[lignin type]-[ethanol : water ratio]-[temperature]-[time] (*e.g.*, KFA-AEL-7/3-140-2).

4.4 Lignin content, yield, and purity analysis

The chemical composition of raw and pretreated poplar wood powder was determined following standard National Renewable Energy Laboratory (NREL) protocols. Briefly, 300 mg of sample was treated with 3 mL of 72% H_2SO_4 for 1 h, diluted to 4% H_2SO_4 with 84 mL deionized water, and autoclaved at 121 °C for 1 h. Lignin metrics were calculated as follows:

$$\text{Lignin content} = m_1/m \times 100\%$$

$$\text{Lignin yield} = m_2/m_1 \times 100\%$$

$$\text{Lignin purity} = m_3/m_2 \times 100\%$$

where m = mass of poplar wood powder (g), m_1 = Klason lignin mass in raw wood (g), m_2 = mass of isolated lignin (g), m_3 = acid-insoluble lignin mass after hydrolysis of isolated lignin (g).

4.5 Lignin and KFA characterization

2D ^{1}H–^{13}C HSQC NMR. 2D ^{1}H–^{13}C HSQC NMR was conducted on a Bruker AVIII HD 500 spectrometer (Bruker Co., Germany). Lignin (~60 mg) was dissolved in 0.6 mL DMSO-d_6. Spectra were acquired with spectral widths of 5000 Hz (^{1}H) and 20 000 Hz (^{13}C), 2048 (^{1}H) and 256 (^{13}C) data points, a relaxation delay of 1.5 s, 128 scans, and a JCH coupling constant of 145 Hz. DMSO-d_6 (δC/δH = 39.52/2.50) served as the internal reference.[52]

^{31}P NMR. ^{31}P NMR was performed on a Bruker AVIII HD 500 spectrometer following a modified literature method. Vacuum-dried lignin (30 mg) was dissolved in 400 μL pyridine-d_5/$CDCl_3$ (1.6 : 1, v/v). Chromium(III) acetylacetonate solution (100 μL, 32.5 mg mL^{-1} in pyridine-d_5/$CDCl_3$) and cyclohexanol internal standard solution (70 μL, 70 mg mL^{-1} in pyridine-d_5/$CDCl_3$) were added. After mixing, 70 μL of 2-chloro-4,4,5,5-tetramethyl-1,3,2-dioxaphospholane (TMDP) was added, and the solution was transferred to an NMR tube.

Gel permeation chromatography (GPC). Weight-average (Mw) and number-average (Mn) molecular weights were determined using an Agilent PL-GPC 220 system (USA) equipped with an Aquagel-OH column (7.5 × 300 mm) and a differential refractive index detector. Samples dissolved in THF were filtered (0.45 μm) and eluted with THF at 1.0 mL min^{-1} (40 °C, injection volume 100 μL).

Fourier transform infrared (FT-IR) spectroscopy. Spectra (4000–500 cm^{-1}) were recorded on a MAGNA-IR 560 spectrometer (Nicolet, USA) using 50 scans at 4 cm^{-1} resolution (KBr pellet method).

Three-dimensional excitation–emission matrix (3D EEM) fluorescence. KFA spectra were acquired on a HITACHI F7000 spectrofluorometer (Japan) with excitation (Ex) from 200 to 800 nm and emission (Em) from 250 to 800 nm (5 nm increments, Ex/Em slit widths 5.0 nm, scan speed 2000 nm min^{-1}).

Elemental analysis (EA). The carbon (C), hydrogen (H), oxygen (O), nitrogen (N), and sulfur (S) contents of lignins and KFA were determined using an Elementar Unicube analyzer (Germany).

X-ray photoelectron spectroscopy (XPS). The chemical states of elements in KFA were analyzed using a Thermo Scientific ESCALAB Xi+ spectrometer (USA).

Fourier transform-ion cyclotron resonance-mass spectrometer (FT-ICR-MS). The sample was analyzed using a Bruker SolariX FT-ICR MS. The ionization source was electrospray ionization (ESI) in negative ion mode. Prior to sample analysis, the instrument was calibrated with 10 mmol L^{-1} sodium formate. After sample detection, internal calibration was performed using dissolved organic matter (with known molecular formulas). Following calibration, the mass error was consistently less than 1 ppm. A volume of 200 μL of the extracted sample was taken for mass spectrometry analysis.

4.6 KFA parameter determination

KFA samples were analyzed for key quality parameters as per the Chinese agricultural standard HG/T 5334-2018; FA content: potassium dichromate oxidation method; potassium (K_2O) content: potassium tetraphenylborate gravimetric method; water-insoluble matter: centrifugation/filtration method; moisture content: vacuum oven drying method; pH: direct measurement using a pH meter. Detailed procedures are provided in the SI. All analyses were performed in triplicate.

Author contributions

Kaixia Liang: writing – original draft, writing – review & editing, investigation, formal analysis, data curation. Jiale Yu: resources, investigation, formal analysis. Jialong Lv: resources, investigation. Qi Tang: validation, investigation. Zhiqian Meng: investigation, data curation. Meng Liu: investigation, formal analysis. Zhimin Chen: resources, investigation. Lihang Guan: resources, investigation. Qinqin Xia: validation, investigation. Shuo Dou: validation, investigation. Xiaoxue Song: supervision, validation, data curation. Haipeng Yu: supervision, writing – review & editing. Yongzhuang Liu: supervision, conceptualization, funding acquisition, writing – review & editing.

Conflicts of interest

The authors declare no competing financial interest.

Data availability

The data supporting this article have been included as part of the supporting information (SI).

Supporting information: Fig. S1–S7, Tables S1–S6, and further experimental details. See DOI: https://doi.org/10.1039/d6im00110f.

Acknowledgements

This work was supported by the National Natural Science Foundation of China (No. 32571981; No. 32330072).

References

1 S. Rostami and A. Azhdarpoor, The application of plant growth regulators to improve phytoremediation of contaminated soils: A review, *Chemosphere*, 2019, **220**, 818–827.
2 C. Mao, J. Byun, H. W. MacLeod, C. T. Maravelias and G. A. Ozin, Green urea production for sustainable agriculture, *Joule*, 2024, **8**, 1224–1238.
3 Y. Yu, W. Yang, L. Yang, Y. Chen and P. Wu, Organic fertilization alleviates Sb toxicity in rice: Insights into Sb speciation, oxidative stress mitigation, and metabolic reprogramming, *J. Hazard. Mater.*, 2025, **500**, 140479.
4 J. Han, B. A. Bryan and Y. Zhang, Strategic cropland reserves can strengthen China's food security, *Nat. Food*, 2024, **5**, 535–538.
5 X. Ge, X. Xiao, Y. Zhang, X. Zhu, C. Chu and B. Chen, Mechanistic insights into the inhibitory role of soil humic components in iron (oxyhydr)oxide formation: From in situ kinetics to molecular thermodynamics, *Environ. Sci. Technol.*, 2025, **59**, 6579–6589.
6 X. Fan, C. Gu, Z. Gao, L. Shen, D. Yan, H. He, X. Yang, Y. Song, M. Ye, F. Wang and X. Jiang, Novel regulatory mechanisms of carboxylesterase by soil organic matter: Correlative insights into enzymatic activation and pollutant degradation via multi–spectral and molecular dynamics approaches, *J. Hazard. Mater.*, 2025, **499**, 140315.
7 H. Li, Q. Zeng, J. Zhu, Y. Zhu and Y. Xu, Integrated production of humic-like acid, fulvic-like acid, and fermentable sugars from industrial xylooligosaccharides manufacturing waste residues via hydrothermal pretreatment, *Ind. Crops Prod.*, 2023, **205**, 117514.
8 D. Cai, Y. Lu, Y. Zhu, D. Wang, J. Shi, L. Liu, J. Li, X. Zhan, W. Zhang and H. Xu, Inducing hour-level humification of Enteromorpha prolifera to fabricate fulvic-like acid fertilizer with Fenton's reagent, *Nat. Commun.*, 2025, **16**, 5860.
9 X. Chen, X. Zhang, H. Chen and X. Xu, Physiology and proteomics reveal Fulvic acid mitigates Cadmium adverse effects on growth and photosynthetic properties of lettuce, *Plant Sci.*, 2022, **323**, 111418.
10 E. Sarlaki, M. H. Kianmehr, N. Marzban, A. Shafizadeh, S. A. F. Sheikh Ahmad Tajuddin, S. Hu, M. Tabatabaei and M. Aghbashlo, Advances and challenges in humic acid production technologies from natural carbonaceous material wastes, *Chem. Eng. J.*, 2024, **498**, 155521.
11 K. Varma, P. K. Jha, S. Mukherjee, A. Singhal and M. Kumar, Provenances, preponderances, and distribution of humic acids and organic pollutants in hydro-geosphere: The co-existence, interaction and isotopic biomarkers in the riverine ecosystem, *J. Environ. Manage.*, 2022, **313**, 114996.
12 Y. Li, F. Li, J. Guo, X. He, X. Gao and M. Wu, Preferential extraction of degraded organic matter and mineral protection of aromatic structures based on molecular marker analysis, *Appl. Geochem.*, 2024, **170**, 106081.
13 N. Li, H. Ma, G. Wang, X. Ma, J. Deng and S. Yuan, Efficient extraction and formation mechanism of fulvic acid from lignite: Experimental and DFT studies, *J. Environ. Manage.*, 2024, **365**, 121650.
14 J. Zhou, H. Ge, Z. Wang, C. Pan, X. Yan, Z. Li, W. Zhang, H. Yan, J. Yan, S. Ren, Z. Lei and H. Shui, Selective upgrading coal-based humic acid to fulvic acid through electrochemical oxidation coupled with hydrogen production, *Sep. Purif. Technol.*, 2025, **359**, 130566.
15 S. Dou, J. Shan, X. Song, R. Cao, M. Wu, C. Li and S. Guan, Are humic substances soil microbial residues or unique synthesized compounds? A perspective on their distinctiveness, *Pedosphere*, 2020, **30**, 159–167.
16 C. Tang, J. Hou, D. Liu, B. Xi, J. Li and H. Yu, Applying fluorescence spectroscopy coupled with Gaussian band fitting to reveal dynamic variation process of humus fractions from riparian soils along an urbanized river, *Sci. Total Environ.*, 2024, **927**, 172193.
17 X. Yang, R. Yan, C. Yang, H. Zhang, H. Lyu, S. Li, T. Liu, R. Li, Y. Yao, W. Li and L. Gao, Soil accelerates the humification involved in co-composting of wheat straw and cattle manure by promoting humus formation, *Chem. Eng. J.*, 2024, **479**, 147583.
18 Y. Long, H. Jin, N. Zhu, J. Zhang, Y. Zhu, L. Chen, Y. Cao, Z. Zhang, Z. Ye and C. Shan, Catalytic and stimulative effects of molecular sieve 13X on promoted humification during composting, *ACS Sustainable Chem. Eng.*, 2025, **13**, 17220–17230.
19 J. Zhou, W. Xu, Z. Wang, R. Hou, W. Chen and Y. Hu, Extraction and characterization of biochemical fulvic acid from cattle manure compost products, *J. Environ. Chem. Eng.*, 2025, **13**, 119394.
20 T. Kunatsa and X. Xia, A review on anaerobic digestion with focus on the role of biomass co-digestion, modelling and optimisation on biogas production and enhancement, *Bioresour. Technol.*, 2022, **344**, 126311.
21 F. Guilayn, M. Benbrahim, M. Rouez, M. Crest, D. Patureau and J. Jimenez, Humic-like substances extracted from different digestates: First trials of lettuce biostimulation in hydroponic culture, *Waste Manage.*, 2020, **104**, 239–245.

22 Y. Shao, M. Bao, W. Huo, R. Ye, M. Ajmal and W. Lu, From biomass to humic acid: Is there an accelerated way to go?, *Chem. Eng. J.*, 2023, **452**, 139172.
23 H. Zhou, Y. Dang, C. Li, X. Chen, Y. Liu, H. Bian, A. Ivanets, J. Zheng, X. He, J. M. García-Mina and X. Su, Conversion mechanism of pyrolysis humic substances of cotton stalks and carbide slag and its excellent repair performance in Cd-contaminated soil, *Chem. Eng. J.*, 2024, **494**, 153147.
24 S. Pan, G. Tian, Z. Su, Z. Shen, J. Zhou, L. Yang, Z. Cui, Z. Zhang, Q. Gao and H. Cai, Analysis of the promotion of lignin conversion to artificial fulvic acid by hydrothermal humification combined with microbial fermentation, *Ind. Crops Prod.*, 2025, **235**, 121695.
25 S. Pan, Z. Zhang, Z. Liu, L. Wu, Q. Gao and H. Cai, The combination of hydrothermal humification and biological fermentation converts straw lignocellulose into artificial fulvic acid, *Int. J. Biol. Macromol.*, 2025, **314**, 144359.
26 Z. Sheng, J. Wang, T. Yang, B. Li and R. Li, Fenton-assisted neutral hydrothermal humification for lignocellulosic biomass to fulvic acid, *Chem. Eng. J.*, 2025, **521**, 166754.
27 D. Wang, X. Chen, J. Zhang, J. Xu, X. Kong, J. Ye, R. Zhang, H. Fan, L. Liu, X. Zhan, Y. Qin, H. Xu, Y. Zhu and D. Cai, Alkaline-thermal synergistic activation of persulfate for sawdust hour-level humification to prepare fulvic-like-acid fertilizer, *Bioresour. Technol.*, 2025, **426**, 132388.
28 D. Cai, X. Kong, X. Zhang, J. Ye, H. Xu, Y. Zhu and D. Wang, Alkali-activated potassium persulfate treatment of sugarcane filter cake for the rapid production of fulvic-like-acid fertilizer, *ACS Sustainable Chem. Eng.*, 2023, **11**, 13678–13687.
29 D. Kong, G. Wang, J. Zheng, X. Zhao, L. Zhang, B. Davronbek, H. Wu, J. Wan and X. Su, Sustainable synthesis of artificial humic substances from bamboo powder by $FeCl_3$-catalyzed low-temperature pyrolysis for cadmium contaminated soil remediation and carbon sequestration, *Environ. Res.*, 2026, **289**, 123319.
30 J. Li, W. Gan, Z. Chen, H. Yang and Y. Wang, Frontier advances in wood science Towards a new departure, *For. Eng.*, 2025, **41**, 1–39.
31 S. Constant, H. L. J. Wienk, A. E. Frissen, P. d. Peinder, R. Boelens, D. S. van Es, R. J. H. Grisel, B. M. Weckhuysen, W. J. J. Huijgen, R. J. A. Gosselink and P. C. A. Bruijnincx, New insights into the structure and composition of technical lignins: A comparative characterisation study, *Green Chem.*, 2016, **18**, 2651–2665.
32 Y. Li, Y. Liu, W. Chen, Q. Wang, Y. Liu, J. Li and H. Yu, Facile extraction of cellulose nanocrystals from wood using ethanol and peroxide solvothermal pretreatment followed by ultrasonic nanofibrillation, *Green Chem.*, 2016, **18**, 1010–1018.
33 H. Liu, X. Chen, S. Ni, Z. Li, N. Liu and Y. Fu, Role of lignin removal on the properties of crude pulp fibers from corn stover via high-temperature formic acid pulping, *Int. J. Biol. Macromol.*, 2025, **287**, 138435.
34 J. Yang, Y. Huang, W. Yang, L. Jiao, S. Zhang and H. Dai, Efficient production of low molecular weight lignin from eucalyptus wood through methanol-alkali system, *Ind. Crops Prod.*, 2024, **207**, 117728.
35 H. Labauze, N. Cachet and B. Benjelloun-Mlayah, Acid-based organosolv lignin extraction from wheat straw: Kinetic and structural analysis, *Ind. Crops Prod.*, 2022, **187**, 115328.
36 Q. Liu and S. Zhu, Fractionation of depectinated sugar beet pulp into cellulose, hemicellulose, and lignin with NaOH/urea/H_2O and ionic liquid, *Int. J. Biol. Macromol.*, 2023, **242**, 124706.
37 R. C. Sun, Lignin source and structural characterization, *ChemSusChem*, 2020, **13**, 4385–4393.
38 Z. You, X. Kang, S. Zhao, T. He, J. Zhang, A. J. Ragauskas, X. Zhuang, J. Pang, X. Song and M. H. Z. Zhang, Developing a new ethylene glycol/H_2O pretreatment system to achieve efficient enzymatic hydrolysis of sugarcane bagasse cellulose and recover highly active lignin: Countercurrent extraction, *Sep. Purif. Technol.*, 2025, **354**, 128564.
39 D. S. Zijlstra, C. W. Lahive, C. A. Analbers, M. B. Figueirêdo, Z. Wang, C. S. Lancefield and P. J. Deuss, Mild organosolv lignin extraction with alcohols: The importance of benzylic alkoxylation, *ACS Sustainable Chem. Eng.*, 2020, **8**, 5119–5131.
40 J. Yang, W. Zhang, Y. Wang, M. Li, F. Peng and J. Bian, Novel, recyclable Brønsted acidic deep eutectic solvent for mild fractionation of hemicelluloses, *Carbohydr. Polym.*, 2022, **278**, 118992.
41 H. Paananen, L. Alvila and T. T. Pakkanen, Hydroxymethylation of softwood kraft lignin and phenol with paraformaldehyde, *Sustainable Chem. Pharm.*, 2021, **20**, 100376.
42 B. Du, Y. Yang, L. Huang, Y. Xie, X. Wang, J. Zhou, X. Ji and L. Shao, From industrial waste to multistage applications: Ultralight lignin-based aerogel with situ vertically oriented structure for photothermal-assisted Pb^{2+} adsorption in wastewater and reuse as efficient output and stability triboelectric materials, *Adv. Sci.*, 2025, **12**, e13337.
43 S. Sutradhar, N. Alam, L. P. Christopher and P. Fatehi, KOH catalyzed oxidation of kraft lignin to produce green fertilizer, *Catal. Today*, 2022, **404**, 49–62.
44 B. Liu, W. Zhang, J. Zeng, N. Gong, G. Ying, P. Li, B. Wang, J. Xu, W. Gao and K. Chen, Acid-catalyzed phenolation of lignin with tea polyphenol: Enhancing uv resistance and oxidation resistance for potential applications, *Int. J. Biol. Macromol.*, 2024, **267**, 131462.
45 X. Peng, S. Gai, K. Cheng and F. Yang, Hydrothermal humification mechanism of typical agricultural waste biomass: A case study of corn straw, *Green Chem.*, 2023, **25**, 1503–1512.
46 G. Zhu, L. Yang, Y. Gao, J. Xu, H. Chen, Y. Zhu, Y. Wang, C. Liao, C. Lu and C. Zhu, Characterization and pelletization of cotton stalk hydrochar from HTC and combustion kinetics of hydrochar pellets by TGA, *Fuel*, 2019, **244**, 479–491.
47 Y. Wang, X. Liu and J. Zhou, Two new 3-D vanadoborates incorporating rare polymeric K-O-K chain or network with photocatalytic properties, *Inorg. Chem. Commun.*, 2024, **167**, 112720.

48 G. Gong, Y. Zhao, Y. Zhang, B. Deng, W. Liu, M. Wang, X. Yuan and L. Xu, Establishment of a molecular structure model for classified products of coal-based fulvic acid, *Fuel*, 2020, **267**, 117210.

49 N. T. Phong, H. Y. Yoon, M. S. Kang, M. Kwon, Y. Lee, J. M. Baik, E. J. Son, K. Jang, D. Han, K. S. Kim and J. Jeon, Ionic liquid-based extraction of fulvic-like substances from wood sawdust: Reproducing unique biological activities of fulvic acids using renewable natural sources, *J. Agric. Food Chem.*, 2024, **72**, 20981–20990.

50 D. Mu, L. Mu, X. Geng, T. A. Mohamed and Z. Wei, Evolution from basic to advanced structure of fulvic acid and humic acid prepared by food waste, *Int. J. Biol. Macromol.*, 2024, **256**, 128413.

51 W. Li, X. Li, C. Han, L. Gao, H. Wu and M. Li, A new view into three-dimensional excitation-emission matrix fluorescence spectroscopy for dissolved organic matter, *Sci. Total Environ.*, 2023, **855**, 158963.

52 Y. Lou, X. Sun, Y. Yu, S. Zeng, Y. Li, Y. Liu and H. Yu, One-pot protolignin extraction by targeted unlocking lignin–carbohydrate esters via nucleophilic addition–elimination strategy, *Research*, 2023, **6**, 0069.